

Multi-layered Multi-Constellation Global Navigation Satellite System Interference Mitigation

Ciro Gioia* | Daniele Borio

Joint Research Centre (JRC)
European Commission
Ispra (VA)
Italy

Correspondence

Ciro Gioia
Via Enrico Fermi 2749,
21027 Ispra (VA), Italy
Email: ciro.gioia@ec.europa.eu

Abstract

Several layers of defense can be implemented in a global navigation satellite system (GNSS) receiver to improve its performance in the presence of interference. These layers include the use of pre-correlation mitigation techniques, post-correlation quality indicators to screen measurements, and fault detection and exclusion (FDE) at the position solution level. This paper provides a characterization of the interactions between these layers of interference mitigation and a measurement quality check. Data collected in the presence of increasing levels of jamming were processed using different interference mitigation techniques, including robust interference mitigation (RIM) and the adaptive notch filter (ANF). A software defined radio (SDR) approach was adopted and measurements were generated by considering five interference-mitigation techniques. Position solutions were then computed using a forward-backward approach for receiver autonomous integrity monitoring (RAIM). Signals from GPS, Galileo, and Beidou were processed and both single and dual-constellation solutions were analyzed. The analysis revealed that interference mitigation allows the receiver to track a larger number of signals even in the presence of high levels of jamming power. This increased measurement availability was then effectively exploited by RAIM techniques to provide more reliable solutions. Measurements from several constellations further improved the reliable availability of the position solutions.

Keywords

jamming, multi-layer defenses, notch filter, RAIM, RIM

1 | INTRODUCTION

Global navigation satellite system (GNSS)-based position, velocity, and time (PVT) information is fundamental for several location based services (LBSs). In this respect, GNSS receivers are key technological enablers of a variety of applications. GNSS receivers must meet several requirements not only for accuracy but also those associated with integrity and resilience to interference. For this reason, significant effort has been devoted to develop robust GNSS devices that can provide a reliable PVT solution in the presence of significant levels of interference and other impairments.

Several layers of defense can be implemented in a GNSS receiver to improve its performance in the presence of interference (Dovis, 2015). These defenses include pre-correlation interference mitigation (Borio & Gioia, 2021), post-correlation measurement screening based on lock indicators (LIs) (Van Dierendonck, 1996), fault detection and exclusion (FDE) (Kuusniemi, 2005), and robust positioning algorithms at the PVT level (Zhang et al., 2020). The use of multiple defense layers increases the robustness of GNSS signal reception and leads to more reliable and accurate PVT solutions even in the presence of strong interference. While the combined use of these approaches can significantly improve receiver performance (Zhang et al., 2020), their interactions and cascading effects have only been marginally investigated in the literature. In particular, the impact of interference mitigation techniques on FDE and receiver autonomous integrity monitoring (RAIM) has been considered only minimally. The goal of this paper is to fill this gap with an experimental analysis of the performance and interactions of these receiver defenses with a specific focus on jamming mitigation techniques and RAIM. Emphasis has been given to the multi-constellation case in which signals from several constellations are combined to improve performance.

The analysis is based on a software defined radio (SDR) approach where GNSS signals contaminated by progressively increasing jamming power were recorded to a disk and analyzed with several different approaches. The signals have been processed using a custom Matlab software receiver that implements different jamming mitigation techniques and RAIM approaches. Interference mitigation techniques include four robust interference mitigation (RIM) approaches and the adaptive notch filter (ANF), which are both pre-correlation defenses (Borio & Gioia, 2021). As post-correlation defense, an LI from the literature (Van Dierendonck, 1996) has been adopted.

In terms of FDE, the forward-backward (FB) approach (Gioia, 2014; Kuusniemi et al., 2007) was considered. This approach exploits the redundancy of measurements used to check for the presence of outliers which are subsequently removed. While FDE techniques can lead to improved performance, they are effective only when a redundant set of measurements is available, for example, in a multi-constellation scenario. In the presence of jamming or interference, one or more (if not all) satellite signals can be lost, thereby reducing the number of available measurements. This condition can compromise the performance of the integrity algorithms. Interference mitigation techniques aim at mitigating this condition by improving the availability of GNSS observations.

The analysis was conducted based on the data sets collected by Borio & Gioia (2021), which have been reprocessed to include FDE. Beidou signals were also considered. Signals from three constellations, including GPS, Galileo, and Beidou, were analyzed; for the multi-constellation solutions, pairs of GNSSs were considered. Three tests were performed independently on two frequencies. For the first two tests, GPS L1 coarse acquisition (C/A), Galileo E1B/C, and Beidou B1C signals were processed. For the third test, Galileo E5B and Beidou B2B signals were analyzed. No data sets with dual frequency signals were recorded; hence the analysis focused on single frequency solutions. These signals have different characteristics, including modulations and primary code lengths, which lead to the differential impact of the interference and mitigation techniques.

The three data sets were processed using different interference mitigation techniques that led to GNSS measurements of varying quality. The observations generated by this method were then used to compute the PVT solution that was coupled with FDE. The solution was computed for single and multi-constellation cases using a weighted least squares (WLS) method. Two different weighting schemes were

used; the first scheme involved weights based on satellite elevation, and the second was based on weights of the different measurements that were computed from the carrier-to-noise power spectral density ratio (C / N_0). For multi-constellation solutions, the inter-system bias between the different GNSSs was considered as an additional unknown in the navigation solution. To verify the reliability of the solution, an FDE block was included in the navigation algorithm. Although this block adds complexity to the baseline PVT computation, it facilitates the detection and exclusion of outliers.

Results from the analysis conducted revealed that interference mitigation can significantly improve the reliable availability of the navigation solution, that is, the number of epochs where not only a PVT solution is available but one that is also considered reliable by the FDE algorithm. Interference mitigation allows the receiver to track a higher number of signals, even in the presence of high jamming levels. This increased measurement availability compared to the case in which mitigation was not implemented and provides additional redundancy that is exploited by the FDE technique. As discussed by Borio & Gioia (2021), time domain RIM techniques are the most effective for the scenarios considered here. When these techniques are used, the average number of measurements rejected by FDE is significantly decreased as compared to a case without mitigation. This is another indication of the benefits of this type of approach.

This analysis also highlights the benefits of multi-constellation solutions with improved position accuracy, availability, and reliability.

The remainder of the paper is structured as follows. A brief description of the pre-correlation mitigation techniques is provided in Section 2. The integrity algorithm is presented in Section 2.3. The setup used for the data collection is described in Section 3 and Section 4 summarizes the experimental results obtained. Finally, Section 5 concludes the paper.

2 | SYSTEM OVERVIEW

A GNSS receiver features several layers of defense against radio frequency (RF) interference and other signal impairments. A schematic representation of the different layers of defense is presented in Figure 1. As shown, the impact of interference can be mitigated at the sample, correlator, and measurement level. In addition to the aforementioned stages, interference can be mitigated at the front-end level working on analog signals before signal quantization (Pärlin & Riihonen, 2020). Analog approaches are not considered in this work; only the layers described in Figure 1 are analyzed.

At the sample level, pre-correlation interference mitigation (Dovis, 2015) operates directly on the samples provided by the receiver front-end. This paper considers the five interference mitigation approaches analyzed by Borio & Gioia (2021)

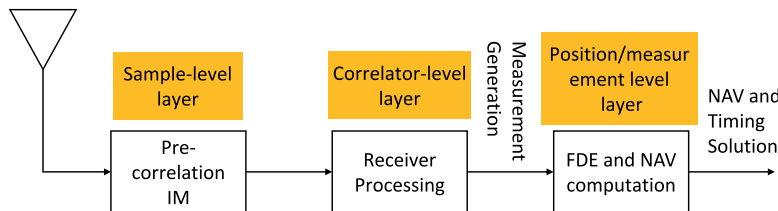


FIGURE 1 Multi-layered GNSS receiver defenses
The interference impact is mitigated at the sample, correlator, and measurement levels.

and briefly discussed in the sections to follow. At the correlator level, metrics such as the C/N_0 and LIs can be monitored to exclude signals that are too weak or too compromised by interference to be useful in the computation of the navigation solution. In this work, we considered the phase lock indicator (PLI) discussed by Van Dierendonck (1996) to screen and exclude signals that were compromised by interference. The PLI is an indicator of signal phase quality with values in the $[-1, 1]$ range and where 1 indicates perfect phase lock conditions. In this work, only signals characterized by a PLI higher than 0.2 were used to generate measurements. Finally, FDE techniques can be implemented to verify the consistency of the measurement set and exclude observations affected by gross errors.

2.1 | Interference Mitigation

In this work, five interference mitigation techniques are considered. Four RIM techniques and the ANF were analyzed along with their interactions with the FDE block. The four RIM techniques considered are as follows (Borio & Gioia, 2021):

- time domain pulse blanking (TDPB), which is a classical approach used to mitigate the impact of pulsed interference. All the time domain samples with an amplitude above a detection threshold, T_h , are set to zero. In this case, $T_h = 3\sigma$, where σ is the total standard deviation of the samples collected in the absence of interference.
- time domain complex signum (TDCS) in which the time domain samples are normalized by their amplitude. The following non-linearity is applied to the input samples, $y[n]$ as indicated in Equation (1):

$$\tilde{y}[n] = \begin{cases} \frac{y[n]}{\|y[n]\|} & \text{for } y[n] \neq 0 \\ 0 & \text{otherwise} \end{cases} \quad (1)$$

- frequency domain pulse blanking (FDPB), where the samples are first brought into the frequency domain through a fast fourier transform (FFT)/discrete fourier transform (DFT) operation. Pulse blanking is then applied in the frequency domain and frequency samples above T_f are set to zero. Finally, the processed samples are brought back in the time domain. This technique is also known as frequency domain adaptive filtering (FDAF) and was analyzed as described by Raimondi et al. (2008).
- frequency domain complex signum (FDCS), where complex signum non-linearity as in Equation (1) is applied to the frequency samples.

Finally, the ANF attempts to track and remove jamming by placing a notch in the correspondence of the most powerful frequency component of the interference term.

A detailed description and analysis of these techniques can be found in Borio & Gioia (2021).

2.2 | Navigation Solution

Both single- and multi-constellation solutions were considered in this work. The PVT solution using signals from a single GNSS was computed using the classical

approach reported by Kaplan & Hegarty (2005). The three GNSSs considered in this study have a similar structure; the most significant difference is related to the time scale adopted, including Global Positioning System time (GPST) for GPS, Galileo system time (GST) for Galileo, and Beidou time (BDT) for Beidou. When using the measurements provided by several GNSSs, there needs to be some accounting for the different time scales. Although the GNSS-to-GNSS time offset is broadcast within the navigation message, it does not consider the local delay introduced by the receiver (Gioia & Borio, 2016). In this study, a multi-constellation solution is computed by considering an additional unknown that represents the offset between the time scales of the GNSSs considered. Therefore, when GPS and Galileo, GPS (GPS) and Beidou, or Galileo and Beidou measurements are used together, the inter-system bias is included in the estimation process as an unknown (Gioia & Borio, 2016).

The navigation solution is obtained using a WLS. Different weighting schemes can be adopted; two weighting functions are analyzed here. The first system is based on the satellite elevation with the *a priori* measurement accuracy computed as the sum of four contributions related to the user ranging accuracy (URA), tropospheric error, ionospheric error, and multipath (Gioia, 2014) as indicated in Equation (2):

$$\sigma_{pr}^2 = \sigma_{URA}^2 + \sigma_T^2 + \sigma_I^2 + \sigma_{mp}^2 \quad (2)$$

where σ_{URA}^2 is computed using the URA value reported in the navigation message. σ_T^2 is computed as indicated in Equation (3) (RTCA Special Committee 159, 2001):

$$\sigma_T^2 = \frac{0.12 \cdot 1.001}{\sqrt{(0.002 + \sin(el)^2)}} \quad (3)$$

where el is the satellite elevation angle. σ_I^2 is computed according to Klobuchar (1987) as shown in Equation (4):

$$\sigma_I^2 = 1 - \frac{R \cdot \cos(el)}{R + HI} \quad (4)$$

where R is the Earth radius and HI is the height of the thin layer in which the electron content is assumed to be concentrated (equal to 350 km). Finally, σ_{mp}^2 is computed as shown in Equation (5) (RTCA Special Committee 159, 2001):

$$\sigma_{mp}^2 = \frac{0.22}{\tan(el)}. \quad (5)$$

For the C/N_0 case, the measurement variance is computed as indicated in Equation (6):

$$\sigma_{pr}^2 = a + b \cdot 10^{\frac{c/N_0}{10}}, \quad (6)$$

where the constants a and b are set equal to 10 m^2 and $150 \text{ m}^2/\text{Hz}$, respectively (Kuusniemi, 2005).

2.3 | Reliability

The integrity problem is fundamental issue for many GNSS applications. While integrity information is usually computed using RAIM (Brown, 1987;

Walter & Enge, 1995) at the receiver level, more general techniques denoted as FDE approaches are available (Kaplan & Hegarty, 2005). FDE can be used to identify and exclude a faulty satellite measurement using a minimum of six visible satellites (in the single constellation case).

FDE techniques are based on the statistical analysis of the residuals. This procedure is typically performed using two different tests. The first test, known as the global test (GT), is carried out to verify the consistency of the measurement set. The GT is based on two hypotheses. While the null hypothesis assumes that the adjustment model is correct and the distributional assumptions are consistent with reality, the alternative hypothesis assumes that the adjustment model is not correct. If this test fails, a second test is performed to identify the outlier, i.e., the so-called local test (LT). The LT exploits the standardized residuals that are assumed to be normally distributed. The LT is also based on two hypotheses. In the first case, no standardized residual exceeds a local threshold, and thus the measurements are not flagged as blunders. If this happens, the solution is declared unreliable because of the inconsistency of the results provided by the GT and LT. If at least one standardized residual exceeds the local threshold, the associated measurement is flagged as a blunder and is rejected.

Several FDE techniques can be obtained by combining GT and LT. In the version considered in this study the FB scheme is implemented.

Most of the FDE techniques that have been developed consider the single fault case (Brown, 1987) in which a single measurement is considered faulty in each epoch. In the presence of interference, this assumption might not be valid because almost all the measurements might be affected by errors. Hence, a modification of the classical algorithms will be needed to take into account the possibility of multiple outliers. This problem has been investigated in the specialized literature, for instance, the report published by Angus (2006) that extended the computation of RAIM protection levels to account for multiple biases. Similarly, a recursive approach was proposed in several publications (Gioia, 2014; Kuusniemi et al., 2007; Petovello, 2003) in which the FDE algorithm excludes measurements until the solution is declared either reliable or unreliable. In this work, the aforementioned iterative approach is used.

2.3.1 | Forward-Backward

The FB approach is a technique that involves the use of both GT and LT (Kuusniemi et al., 2007). In our study, two additional checks were considered. In the first section of the algorithm, i.e., the forward phase, a geometry check is performed to screen out bad geometries and verify that the geometry of the system is sufficiently robust to support integrity. If this proves to be the case, the GT is performed to verify measurement consistency. If the GT declares that the measurement set is inconsistent, the LT is carried out to identify the blunder. To avoid erroneous rejections, an additional check is introduced after the LT. This additional test is based on the correlation coefficient and verifies that the measurement flagged as a possible blunder will be excluded only if it cannot be correlated with other observations (Hewitson & Wang, 2006). The forward phase is performed recursively until no additional erroneous measurements are found and the solution is declared either reliable or unreliable. If the solution is declared reliable and more than one measurement has been excluded, the backward phase is exploited to reintroduce observations that may have been incorrectly excluded. The second part of the FB is based only on the GT. If the measurement set that includes one of the rejected

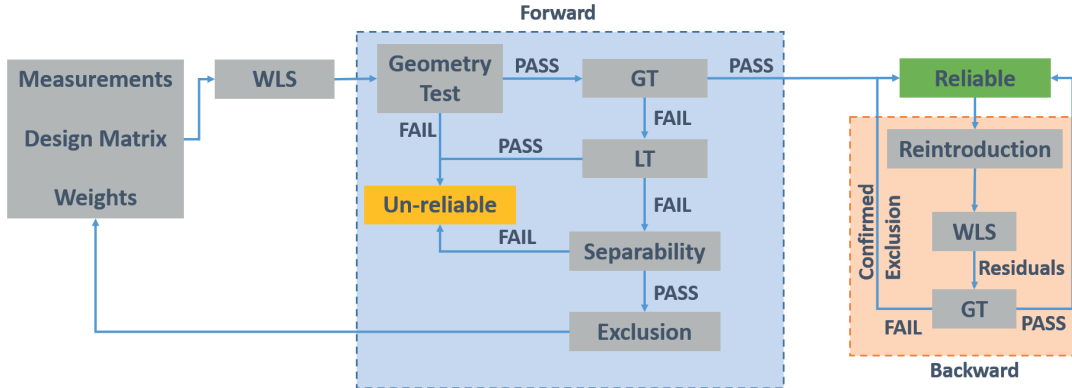


FIGURE 2 Diagram of the FB algorithm

measurement passes the GT, the rejected measurement is retained to compute the final PVT solution. The diagram of the FB algorithm is shown in Figure 2.

2.4 | Performance Indicators

The performance of the different configurations that considers several layers of defense has been evaluated in terms of the following parameters:

- solution availability, defined as the percentage of time during which the solution can be computed.
- reliable solution availability, defined as the percentage of time during which the solution can be computed and the integrity monitoring check can be passed.
- number of excluded satellites as a function of the processing epochs. In addition, the average number of excluded satellites has been computed using a moving window of 30 seconds. The epochs declared as unreliable were not considered in the computation of the average value.
- position error, i.e., the standard deviation of the horizontal position error that was computed.

3 | EXPERIMENTAL SETUP

To assess the interaction between the different layers of interference mitigation, the data used by Borio & Gioia (2021) were considered and reprocessed to include PLI monitoring and FDE. These data were collected in a dedicated experimental setup that included a shielding box that contained a GNSS jammer. The output of the shielding box was connected to a variable power attenuator that was used to simulate different levels of jamming power. Signals from three constellations were collected. Three specific tests were conducted, including Tests 1 and 2 on the L1 frequency and Test E5B in the E5B band with a center frequency equal to 1207.14 MHz. A summary of the signals and frequencies involved in the three tests is provided in Figure 3. For Tests 1 and 2, GPS L1 C/A, Galileo E1B/C, and Beidou B1C were considered. In each test, a single frequency solution was considered. For the third test (Test ESB), Galileo E5B and Beidou B2B signals were analyzed.

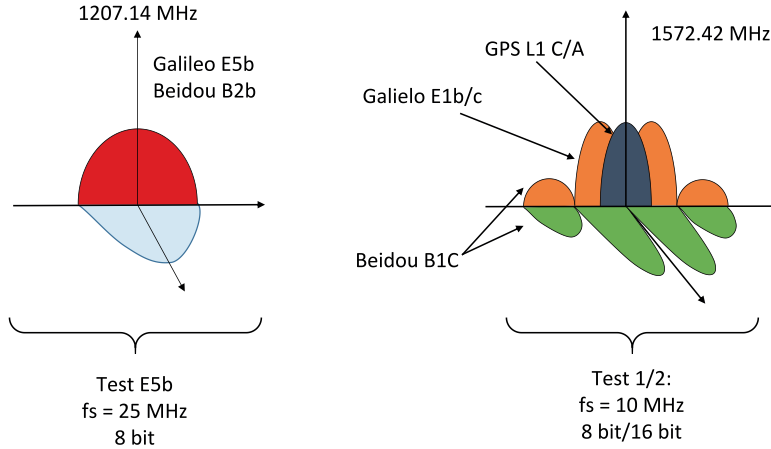


FIGURE 3 Signals and frequencies considered for the different tests

TABLE 1
Signal Characteristics and Parameters Used for the Tests

Parameter	Test 1	Test 2	Test E5B
Sampling Frequency	10 MHz	10 MHz	25 MHz
Centre Frequency	1575.42 MHz	1575.42 MHz	1207.14 MHz
GPS code Period	1 ms	1 ms	
Galileo Code Period	4 ms	4 ms	1 ms
Beidou code Period	10 ms	10 ms	1 ms

Depending on the test, the jammer power was varied in each fixed time interval of 20, 30, and 8 seconds for Test 1, Test 2, and Test E5B, respectively. The jamming signal at the output of the variable attenuator was combined with clean GNSS components collected from a roof-top antenna. In this way, it was possible to collect GNSS signals affected by variable levels of jamming power in a controlled environment. Additional details on the experimental setup can be found in Borio & Gioia (2021).

The collected signals are characterized by different modulations which are affected differently by interference and mitigation techniques. Beidou signals were not considered in our previous work (Borio & Gioia, 2021). The signals considered for the different tests and the main processing options, including sampling frequency, code duration are summarized in Table 1. The main characteristics of the jamming signals and the attenuator parameters are shown in Table 2. These parameters includes the sweep period and the jammer center frequency.

The table also includes the spectral separation coefficients (SSCs) (Betz, 2001; Betz & Kolodziejki, 2009; Borio et al., 2006) estimated for the different jamming signals before receiver front-end saturation. SSCs quantifies the impact of an interfering signal on the effective C/N_0 of the different useful GNSS received signals (Betz & Kolodziejki, 2009; Borio et al., 2006). Detailed information of the jamming to noise power ratio (J/N) profiles for the three tests can be found in Borio & Gioia (2021). The SSCs presented in Table 2 provide indications of the reduction of C/N_0 as a function of the J/N .

A GNSS receiver correlates the input samples with local replicas of the GNSS signal codes and carriers. This operation is equivalent to a filtering process that reduces the impact of interference. Since GPS, Galileo, and Beidou adopt different modulations and integration times, the local replicas used at the receiver side have different characteristics and interference will have different effects. For this reason,

TABLE 2

Characteristics of the Jamming Signals and of the Experimental Setup used for the Tests

Parameter	Jammer 1 - on L1	Jammer 2 - on L1	Jammer 1 - on E5B
Sweep period	9.1 μ s	6.3 μ s	9.1 μ s
Sweep range	36.4 MHz	20.3 MHz	45.7 MHz
Centre Frequency	1553.22 MHz	1575.5 MHz	1213.5 MHz
Attenuation Step	1 dB	1 dB	0.25 dB
Attenuation Time Interval	20 s	30 s	2 s
Analog GPS SSC	$1.04 \cdot 10^{-7}$ [Hz $^{-1}$]	$1.51 \cdot 10^{-7}$ [Hz $^{-1}$]	Not applicable
Analog Galileo SSC	$1.59 \cdot 10^{-7}$ [Hz $^{-1}$]	$1.98 \cdot 10^{-7}$ [Hz $^{-1}$]	$1.01 \cdot 10^{-7}$ [Hz $^{-1}$]
Analog Beidou SSC	$1.82 \cdot 10^{-7}$ [Hz $^{-1}$]	$2.43 \cdot 10^{-7}$ [Hz $^{-1}$]	$1.01 \cdot 10^{-7}$ [Hz $^{-1}$]
Saturation Epoch	300 s	300 s	350 s

SSCs are provided in Table 2 for the different GNSSs considered in this paper. SSC theory is valid only for receivers working in a linear mode, i.e. before front-end saturation. The values presented in Table 2 were estimated before receiver saturation. Saturation epochs provided in the final row of Table 2 were estimated from the J/N curves described in Borio & Gioia (2021).

4 | EXPERIMENTAL RESULTS

The combination of the three levels defenses discussed above, the use of GPS, Galileo, and Beidou signals, and two navigation solution approaches (single and multi-constellation cases) with and without RAIM led to a total of more than 80 processing configurations; these are summarized in Figure 4. Given the large number of combinations, only sample results representing the most relevant configurations are presented. To evaluate the impact of the PLI, only the configuration without additional mitigation strategies was considered both with and without such indicator. All the other configurations adopt the PLI.

The first performance indicators considered were those related to availability and reliable availability. As shown in Figure 5, these two metrics obtained for single constellation solutions were analyzed using Test 1. This test is characterized by an increasing jamming power that leads to front-end saturation after about 400 seconds from the start of the test. After 700 seconds, the level of front-end saturation becomes so high that no mitigation techniques will be able to enable receiver operations and thus no measurements will be produced. For this reason, only the first 700 of the test are considered.

The solution availability was considered as shown in the upper part of Figure 5. As shown, Beidou features the highest availability; this is due the processing strategy adopted and to its specific signal characteristics. The primary code duration of a Beidou B1C is 10 ms. Frequency domain techniques are implemented considering FFTs on data blocks with duration equal to the code length. Thus, for Beidou, longer data blocks are used for the FFT compared to GPS and Galileo. While this provides a better frequency resolution and improves the interference mitigation performance, the assessment of the best FFT data duration for interference mitigation is beyond the scope of this paper. One part from the first case shown at the left of Figure 5 was generated without PLI; in all the other cases, measurement

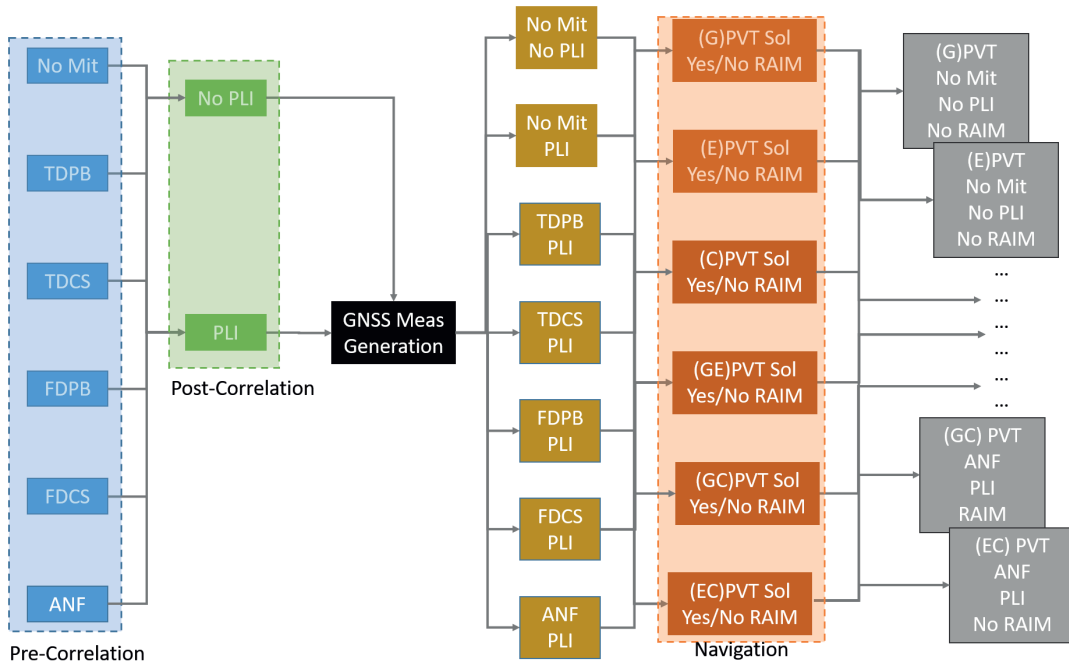


FIGURE 4 Summary of the combinations of multi-layer defenses and the resulting processing configurations

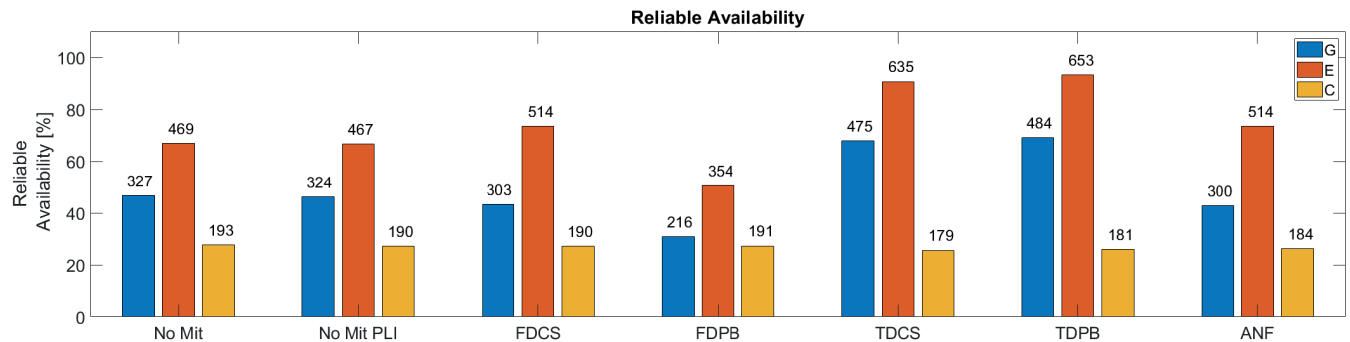
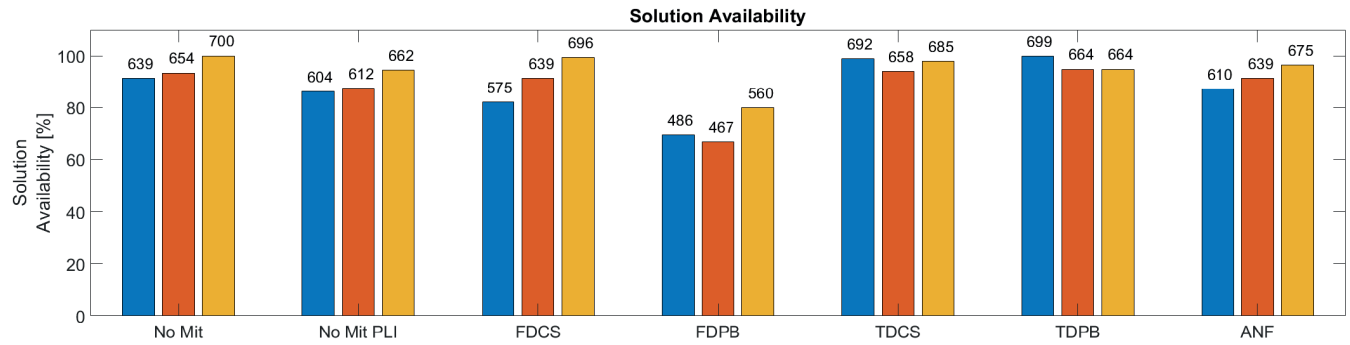


FIGURE 5 Availability and reliable availability for single constellation cases Test 1 and weights based on satellite elevation.

generation was mainly limited by the PLI. For this reason, in the first case, all the 700 epochs considered for the test led to a position solution for the Beidou-only configuration. However, this solution was affected by gross errors that were not excluded in the solution availability analysis. Reduced availability was found for both GPS and Galileo because of the secondary screening that was performed on

the measurements. If the pseudoranges were outside a predefined plausibility interval, they were not included in the measurement set.

The use of time domain RIM slightly improves the overall availability whereas techniques such as FDPB ultimately degrade it. This result is in agreement with the findings discussed by Borio & Gioia (2021). In this case, the jamming signal is mainly concentrated in the time domain where it is perceived as a sequence of pulses, rendering frequency domain interference mitigation techniques ineffective. Moreover, in the FDPB case, the detection threshold, T_f , is too conservative and performance degradation was observed.

The reliable availability was analyzed as shown in the bottom box of Figure 5. In this case, the reliability and quality of the solutions were taken into account. In the scenario considered in Test 1, Beidou solutions were the least reliable with fewer than 200 reliable epochs. This is because of the presence of two Beidou signals which were systematically affected by gross errors. These signals came from low elevation satellites (lower than 10 degrees). Moreover, after approximately 150 epochs from the start of the experiment, loss of lock occurred on one of the Beidou signals; the number of the remaining measurements was then insufficient to check the reliability of the solution. This justifies the reduced number of reliable epochs declared for Beidou compared with the other GNSSs.

In this experiment, Galileo achieved the best performance with reliable availability above 60% for all cases except FDPB. As already discussed, this approach will lead to performance degradation; this is clearly visible in Figure 5. Time domain processing is the most effective. Reliable availability values above 90% were obtained for the Galileo case. For the type of jamming signal considered in this test, the ANF cannot significantly improve the receiver performance.

Availability and reliable availability were analyzed for the dual-constellation case shown in Figure 6. The benefits of using dual-constellation solutions clearly

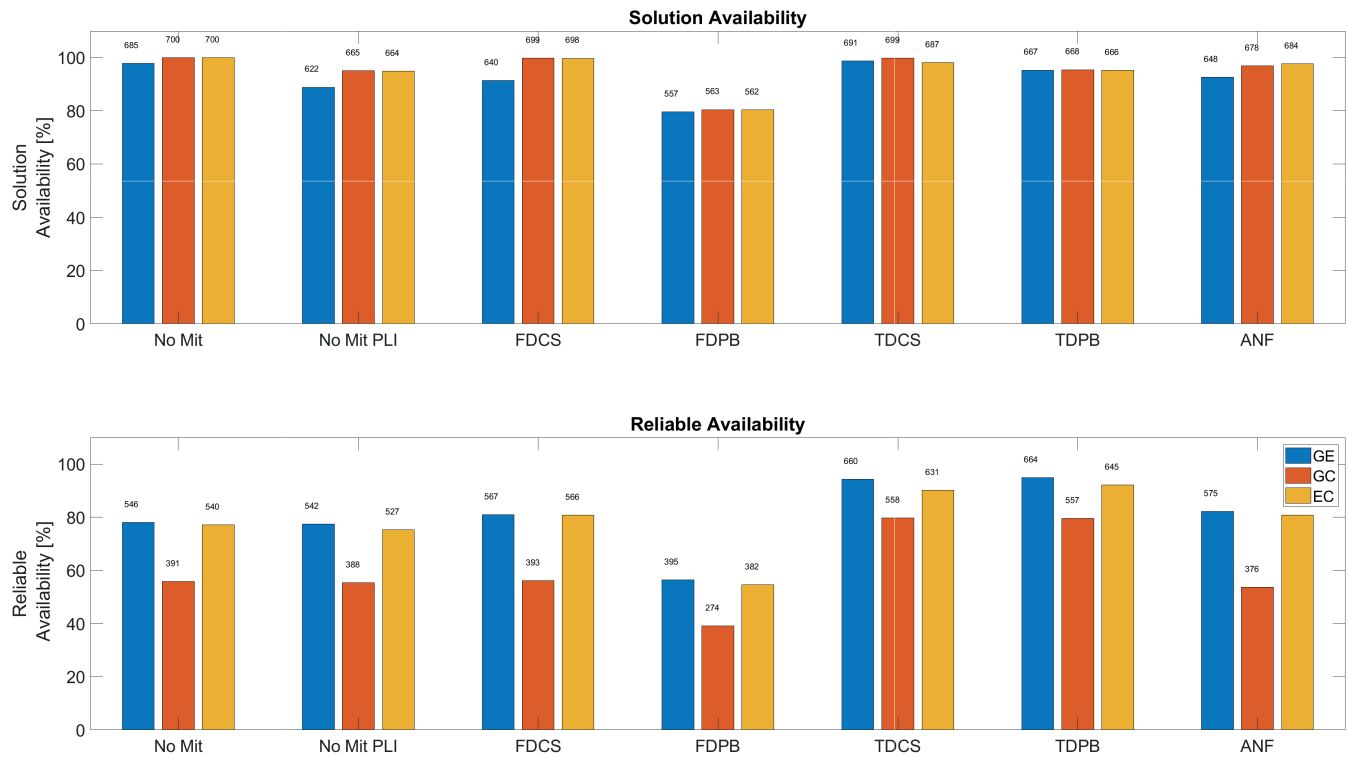


FIGURE 6 Availability and reliable availability for the dual-constellation cases Test 1 with weights based on satellite elevation.

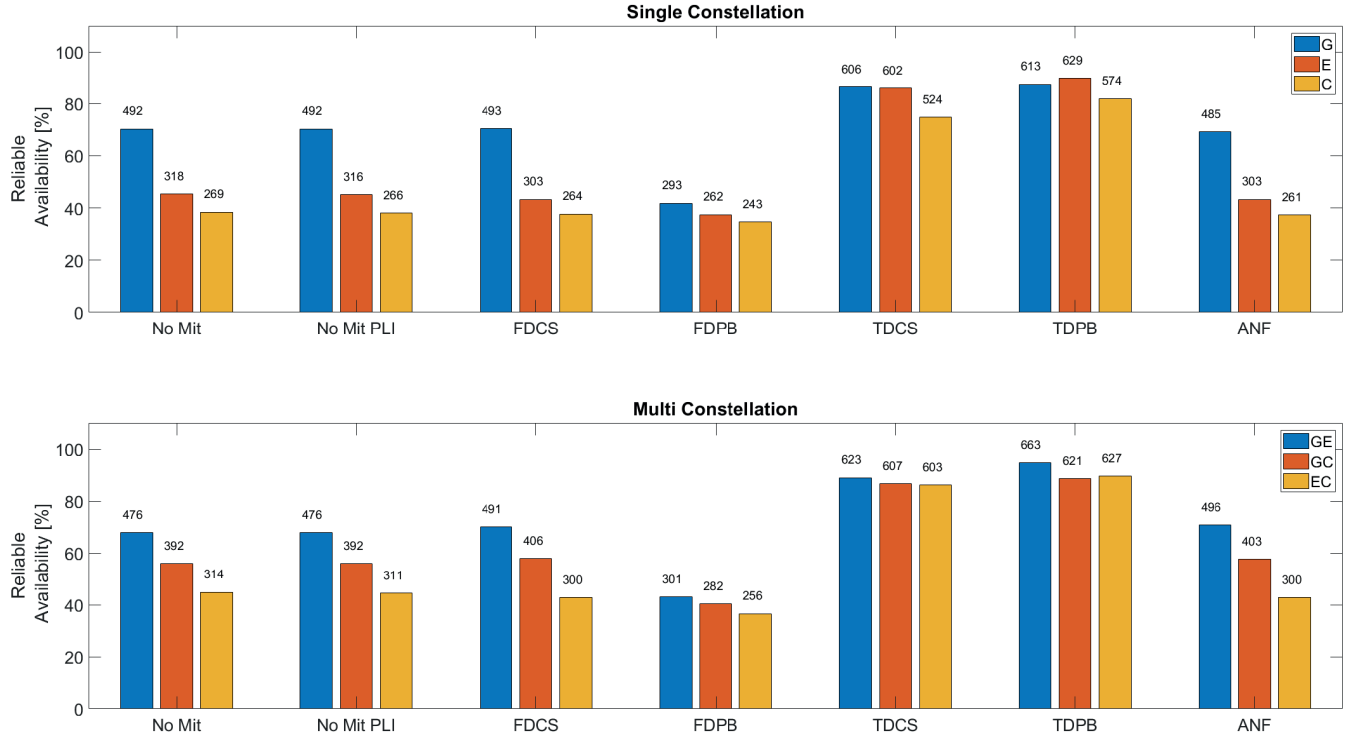


FIGURE 7 Reliable availability for Test 1 using weights based on C/N_0
Upper box: single constellation cases; lower box, dual-constellation cases.

emerge from the findings shown in this figure. As shown, the number of available and reliable epochs increased in all cases. Measurements from two constellations improve the redundancy of the system and present the possibility of checking the reliability of the solution. As shown in the bottom part of Figure 6, one can conclude that most reliable solutions are obtained using the Galileo measurements. This is a consequence of the reliability of the Galileo measurements, as was also observed for the single constellation case. When time domain RIM and Galileo measurements are used, it is possible to obtain reliable position solutions for nearly the entire duration of the test. As in the previous case, no significant improvement in reliability was observed using the ANF.

Similar results were obtained using weights based on the C/N_0 . The reliable availability values obtained for the different configurations considered in Test 1 are shown in Figure 7. In the upper box, the results related to the single constellation cases are considered; in the lower box, the dual-constellation solutions were analyzed. Also in this case, the highest level of reliable availability was obtained when time domain mitigation techniques were applied. A small increase was observed when passing from single to dual constellation solutions. The configuration with the highest level of reliable availability was the one that used GPS and Galileo together with the TDPB. In this case, 663 epochs were declared reliable by the integrity algorithm. The average number of excluded measurements for the single constellations cases is reported in Table 3. The findings presented in the table reveal that the largest values resulted from the Beidou configurations. This is due to the presence of two satellites at very low elevation that were consistently excluded. For GPS and Galileo, the configuration with the largest value was the one that featured the adaptive notch filter. With respect to the no mitigation cases, a very small reduction of the average number of exclusions was noted when PLI was applied. This is because of the exclusions performed by the PLI block. The average

TABLE 3
Mean Number of Exclusions

GNSS	No Mit	PLI	FDCS	FDPB	TDCS	TDPB	ANF
GPS	0.067	0.066	0.049	0.036	0.059	0.061	0.073
Galileo	0.071	0.071	0.107	0.031	0.021	0.027	0.107
Beidou	0.474	0.467	0.469	0.457	0.458	0.461	0.453

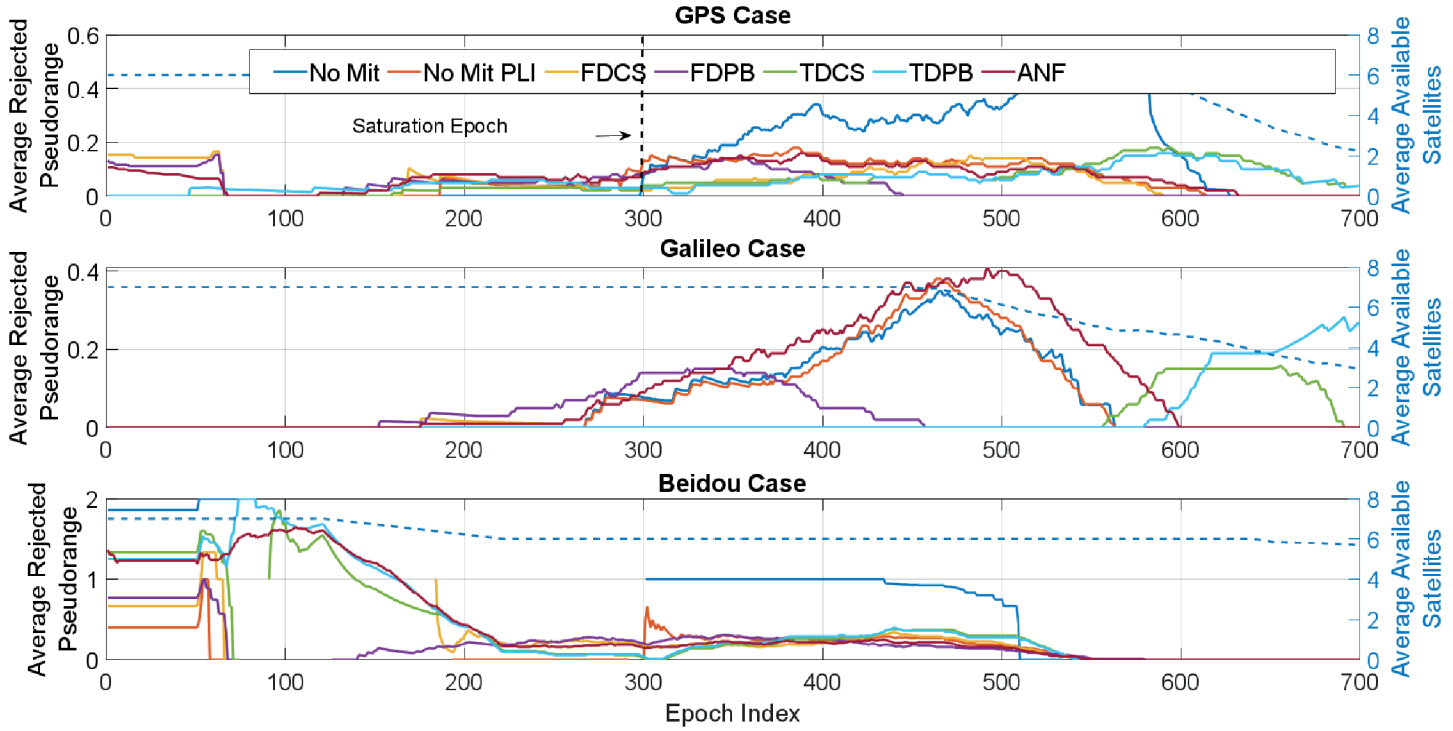


FIGURE 8 Average number of excluded pseudoranges on a 30 second window as function of time
Single constellation cases using elevation dependent weights; Test 1, weights based on satellite elevation.

number of excluded satellites as a function of the epoch index is shown in Figure 8 and Figure 9 for the single and multi-constellation solutions, respectively.

Single-constellation cases are considered in Figure 8. GPS, Galileo, and Beidou are shown in the upper, middle, and lower boxes, respectively. For GPS and Galileo, only a very small number of measurements were excluded during the first part of the test. In the Galileo case, no exclusions were performed during the first 150 seconds of the experiment. By contrast, more exclusions were performed for Beidou from the beginning of the test; an average of two satellites were excluded for each epoch. This phenomena was already discussed at the beginning of the section. In the remaining parts of the test, the average number of exclusions increases as the jamming power increases for all the three single-constellation cases. This is because the increased jamming power affects more measurements, and these are progressively excluded. After approximately 500 seconds, the PLI begins to exclude measurements because of the high jamming power. This led to reductions in the number of available satellites and diminished redundancy. With fewer measurements, RAIM is less effective and the average number of rejected pseudoranges is progressively reduced.

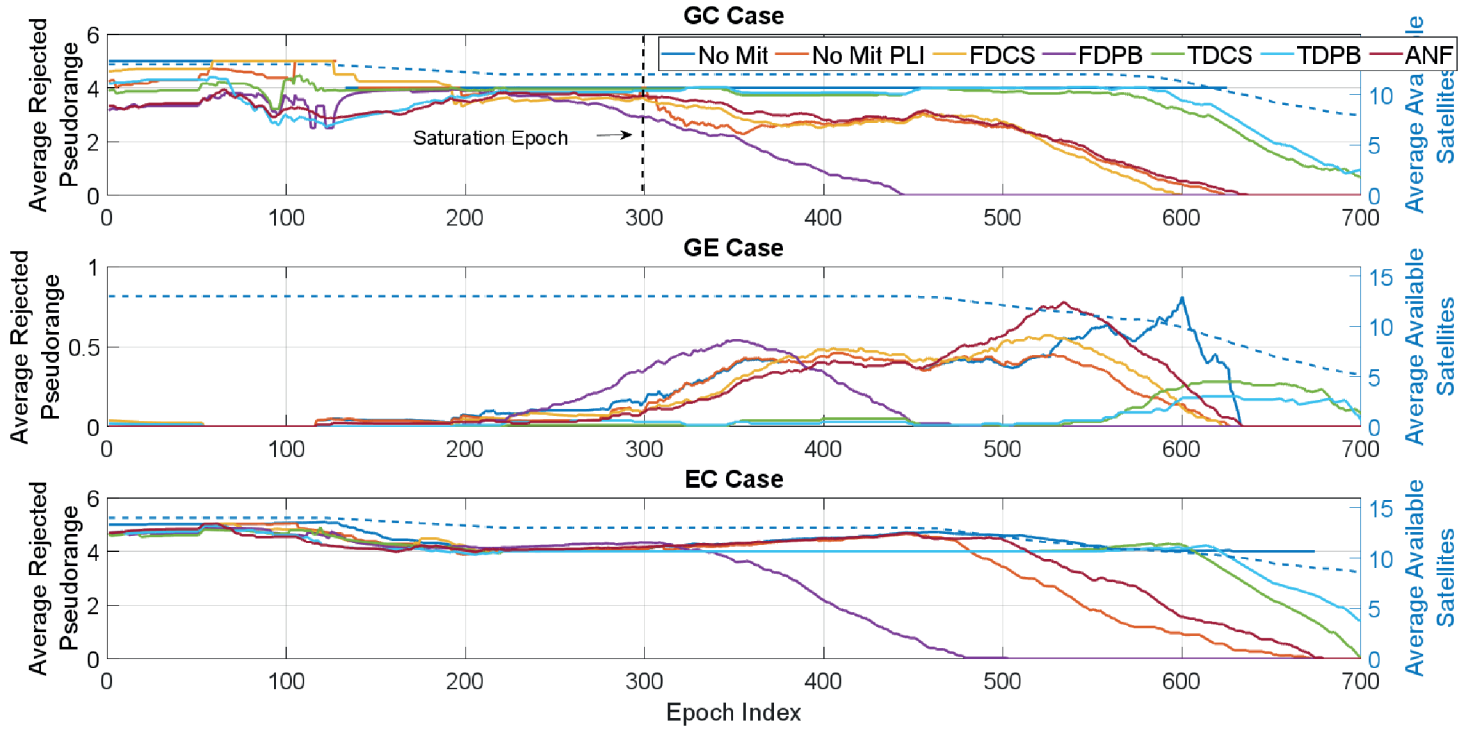


FIGURE 9 Average number of excluded pseudorange on a 30 second window as function of time
Multi-constellation cases using elevation-based weights; Test 1, weights based on satellite elevation.

The comparison between single- and multi-constellation cases revealed that while the behavior of the average number of excluded satellites was similar, the increased redundancy produced using measurements from different GNSSs allows for a higher number of exclusions, thereby improving the performance of the FDE technique.

To assess the relative impact of the different weighting schemes, the average number of excluded satellite measurements as a function of the epoch index obtained using weights based on C/N_0 is shown in Figure 10. To avoid the repetition of similar findings, only results relative to the dual-constellation configurations are shown.

The results shown in the figure reveal that similar findings were observed when using C/N_0 -based weights. For the configurations using Beidou, at least three satellites were excluded from the beginning of the test. This finding is consistent with those observed using satellite elevation-dependent weights. For the GPS plus Galileo case, no exclusion is performed during the first 150 seconds of the experiment. After this time, the average number of exclusions increased corresponding to increases in the jamming power. The number of exclusions also decreases as the redundancy of measurement begins to decrease as well.

The standard deviations of the horizontal positioning errors for the single- and multi-constellation configurations are reported in Figure 11 and Figure 12, respectively. Standard deviations were computed using for each configuration using only epochs declared as reliable. The standard deviations of the horizontal positioning errors that consider only the common reliable epochs are shown in Figure 13. The first group of bars indicates the standard deviations of the horizontal error for the configurations with RAIM activated. Thus, standard deviations were computed for position solutions obtained with the measurements

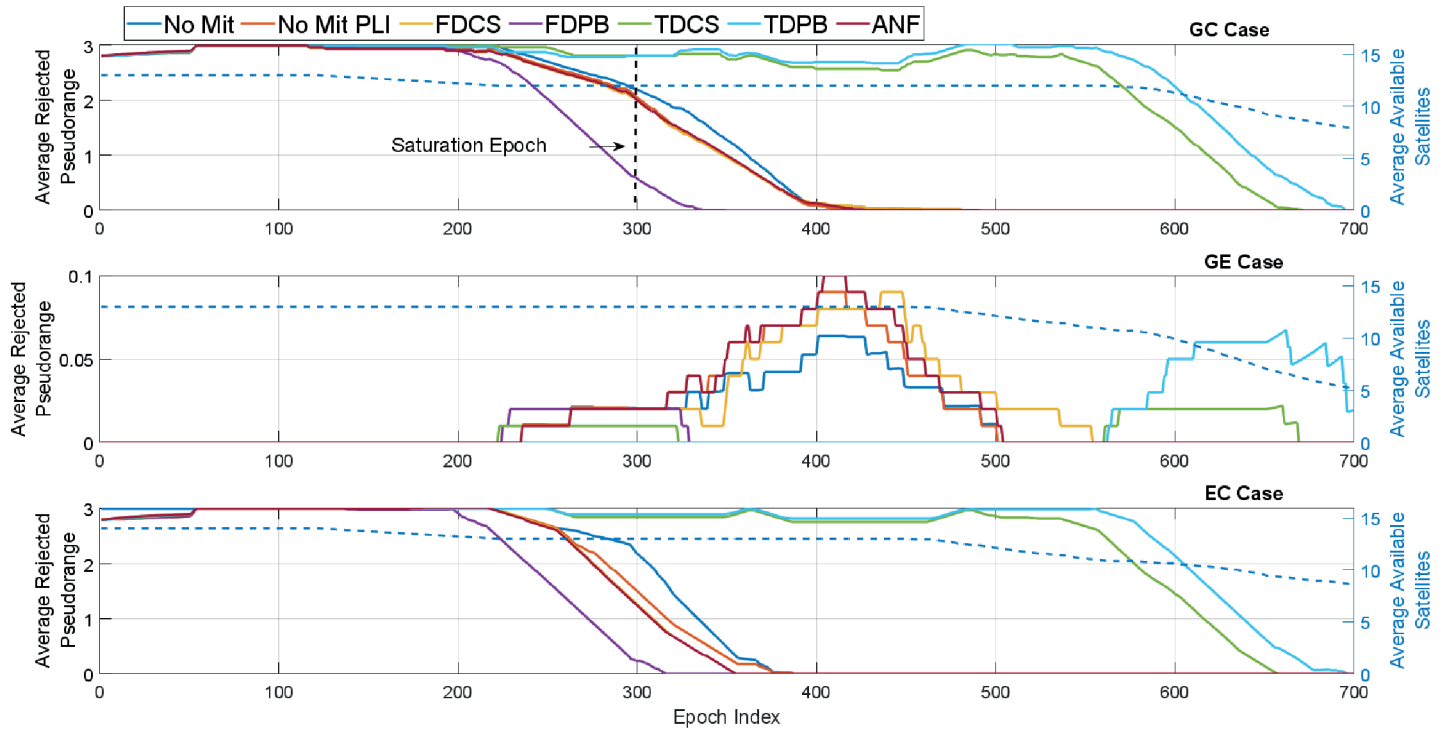


FIGURE 10 Average number of excluded pseudoranges in a 30 second window as function of time

Multi-constellation cases using C/N_0 -based weights, Test 1.

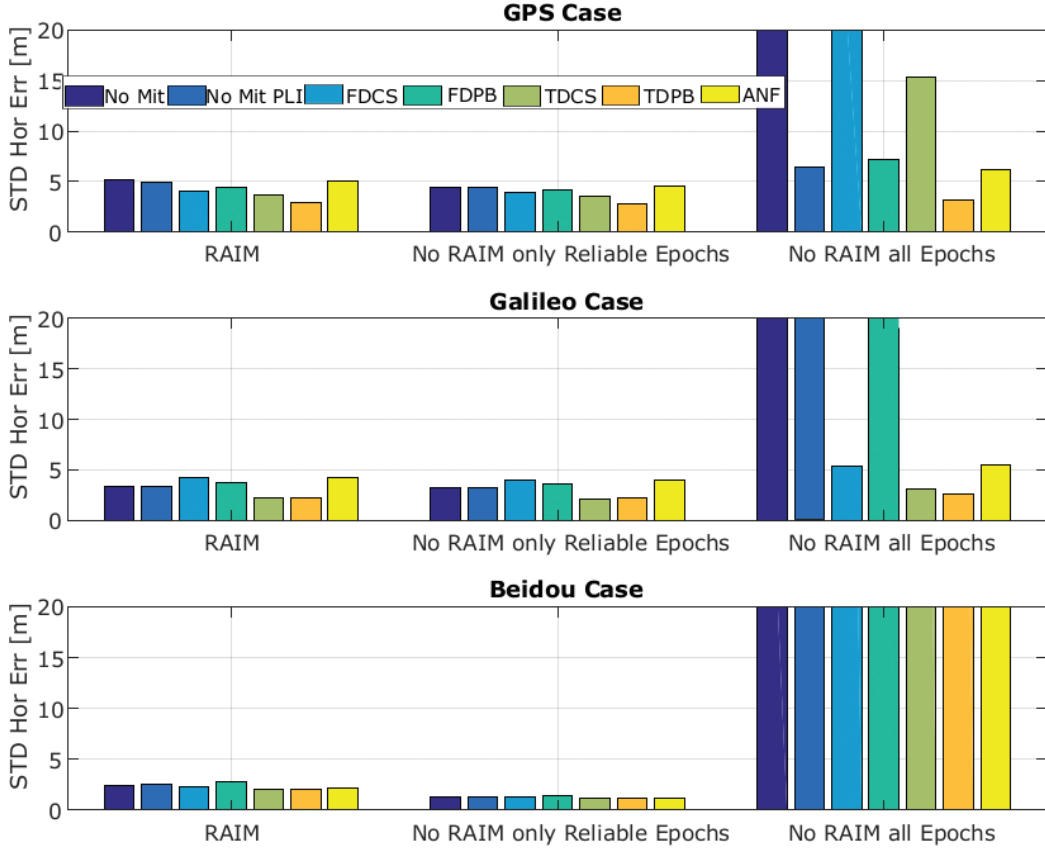


FIGURE 11 Standard deviations of the horizontal positioning errors
Single-constellation cases, Test 1, weights based on satellite elevation.

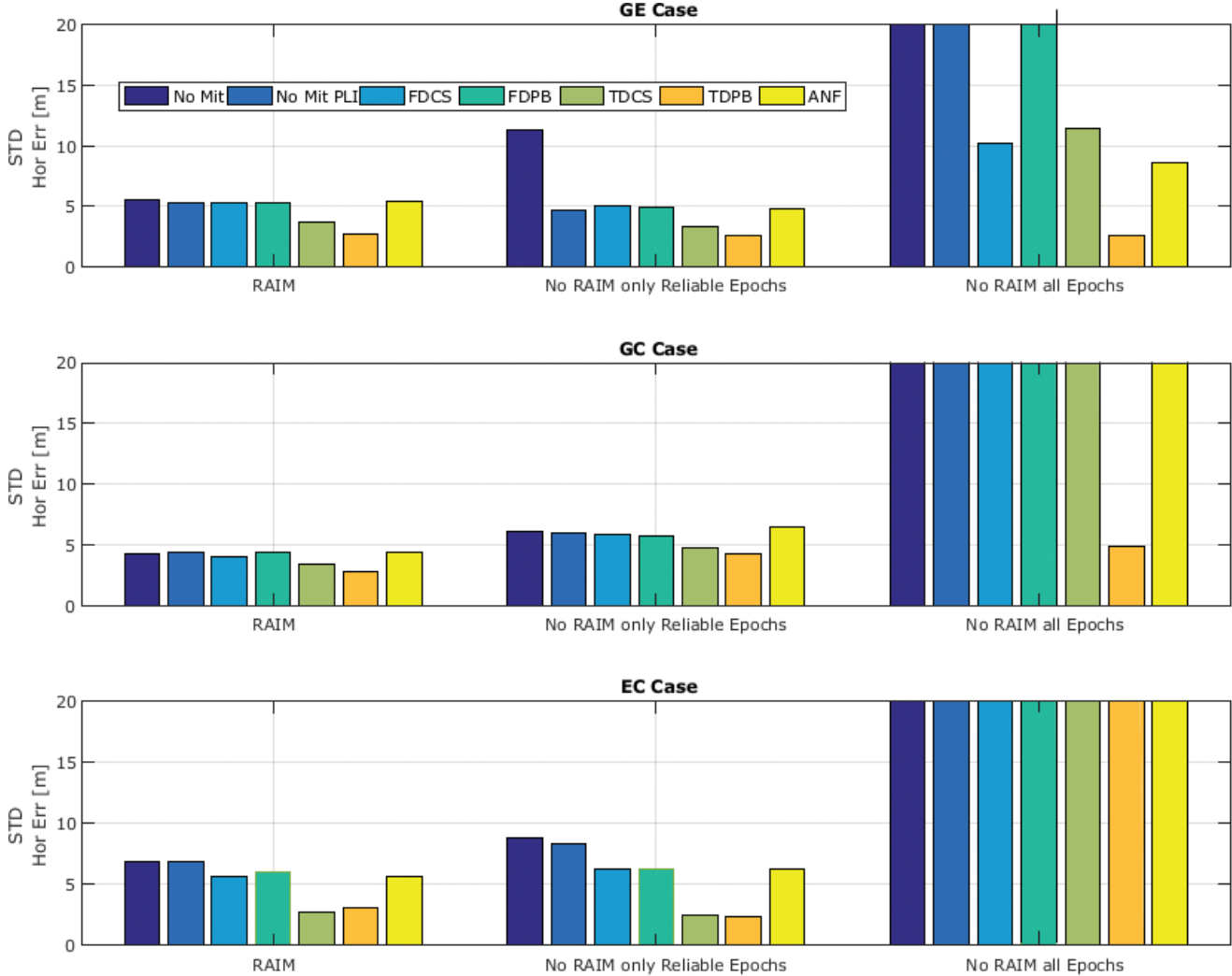


FIGURE 12 Standard deviations of the horizontal positioning errors
Multi-constellation cases, Test 1, weights based on satellite elevation.

selected by RAIM and considered only reliable epochs. For the second group of bars, the standard deviations were computed for the configurations without RAIM, i.e., without performing measurement exclusions, but considering only reliable epochs. Finally, for the third group of bars, the standard deviations were computed for the configurations without RAIM and considered all epochs. The impact of FDE was evident for all configurations. The standard deviation of the horizontal positioning error was strongly reduced compared to the case without RAIM. When considering the single-constellation cases, the configurations of the Beidou-only case display lower values but also the lower reliable availability. The impact of RAIM is even more evident in the multi-constellation cases. A comparison of the results of single- and multi-constellation cases indicates that while the standard deviation values are larger than in the single-constellation cases, the reliable availability of the multi-constellation configurations almost doubles compared to the single GNSS case. The configurations with the lowest values are those that implement time domain mitigation techniques. The synergy between interference mitigation and RAIM leads to standard deviation values on the order of approximately 3 meters (for the GC case) with a reliable availability

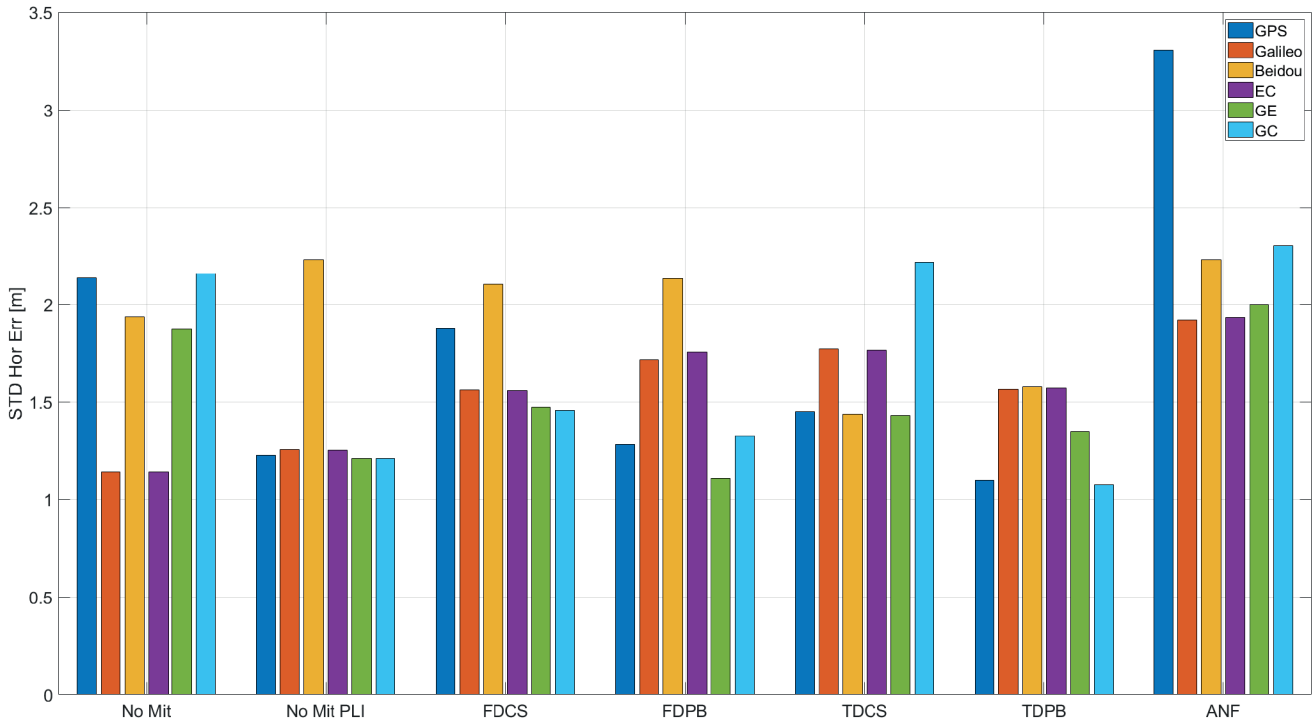


FIGURE 13 Standard deviations of the horizontal positioning errors
Test 1 considering only common reliable epochs, weights based on satellite elevation.

of approximately 80%, which will permit accurate positioning in the presence of strong interference.

Considering only the common reliable epochs, all the configurations show very similar performance with differences on the order of one-half meter. In some cases, small improvements using dual-constellation solutions were observed. The comparison performed using only common reliable epochs penalizes the dual-constellation cases that can provide a reliable solution even in the presence of strong interference, as this leads to a flattening of the performance of the different configurations. The configuration with the lowest value is the one that uses GPS and Galileo together and applies TDPB mitigation.

Results similar to that discussed for Test 1 were obtained for Test 2. These results are omitted to avoid repetition of similar findings.

The data set used for the E5B/B2b test was collected in early 2019, before the completion of the Beidou constellation and with a mix of second- and third-generation signals. For this reason, only a limited number of signals (i.e., five Galileo E5B and three B2b signals) were included in the data set. Given these conditions, it was possible to analyze two specific cases, the Galileo single-constellation solution and the Galileo-Beidou dual-constellation configuration. Because two weighting schemes provided similar results, only the elevation-based case is presented in the text to follow.

The availability and reliable availability of these two solutions are described in Figure 14 for the different configurations, both with and without interference mitigation. The inclusion of the three Beidou measurements significantly improved the reliable availability of the final solution and documented the benefits of multi-constellation configurations, even those with a limited number of observations.

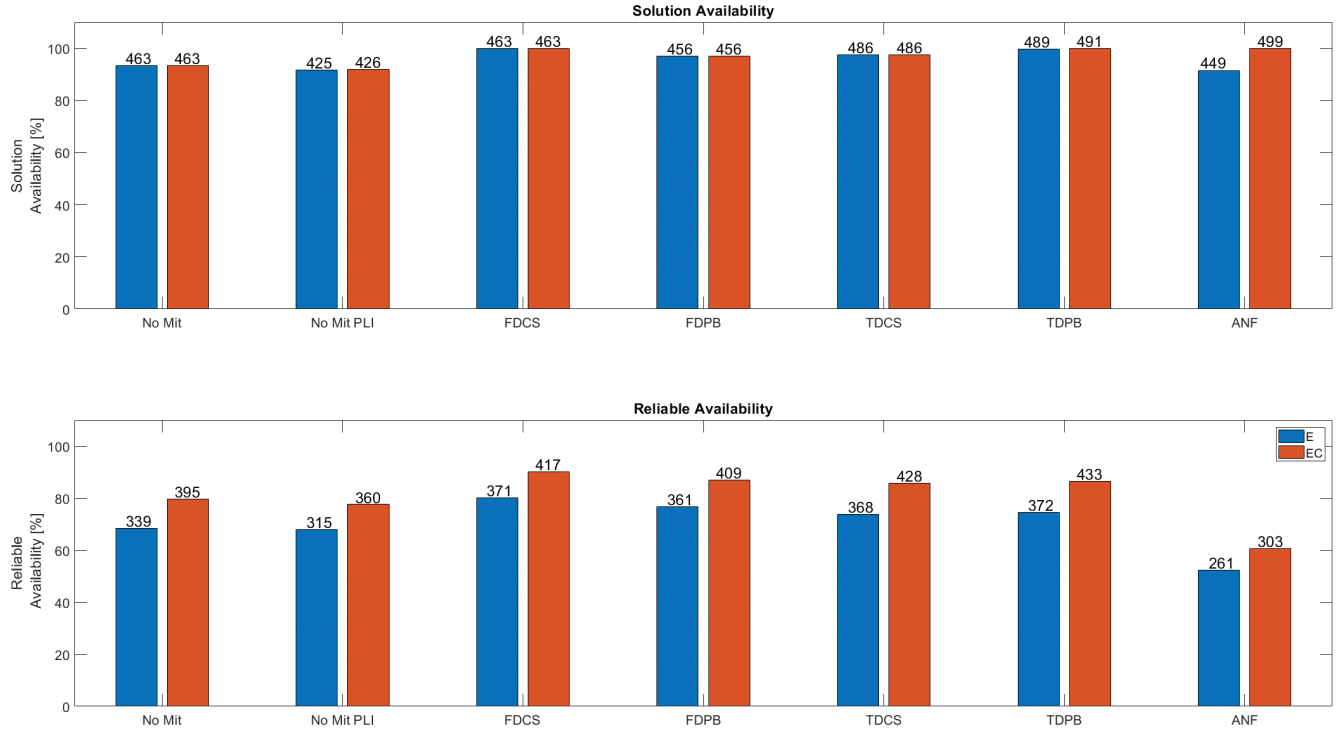


FIGURE 14 Availability and reliab-constellation Galileo-Beidou solutions Test E5B.

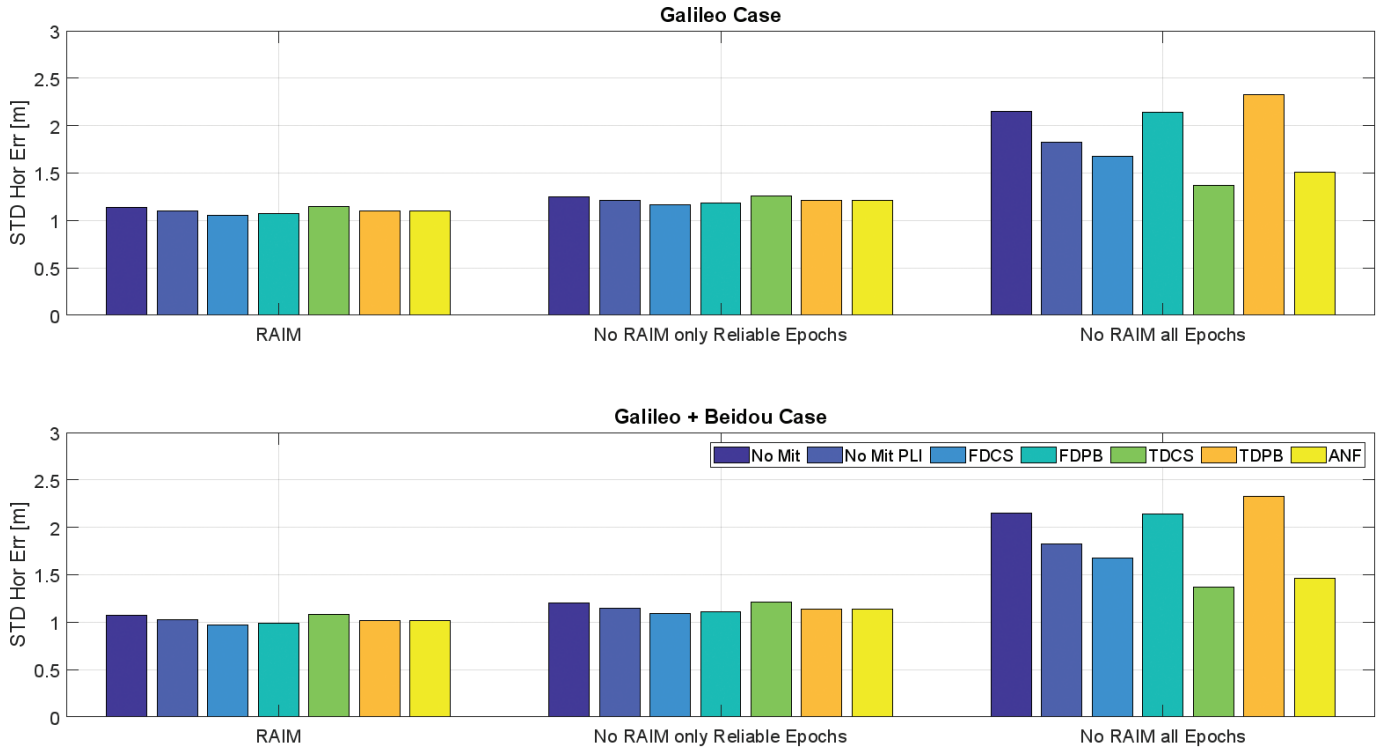


FIGURE 15 Standard deviation of the horizontal positioning errors for Test E5B

The standard deviation of the position solutions obtained for Test E5B is shown in Figure 15. The standard deviations are significantly lower (by approximately a factor of 5) compared to Test 1 in which signals from the L1 frequency were used. This clearly shows the benefits of using wide-band GNSS modulations for this

purpose. These results clearly reveal the positive interaction between the different layers of interference mitigation.

5 | CONCLUSIONS

This paper investigated the cascading effects of different layers of defense against interference and jamming. In particular, the interaction between pre-correlation interference mitigation techniques and FDE approaches was evaluated in a multi-constellation scenario in which pairs of three GNSS constellations were considered. Of note, several tests were performed in which GNSS signals were collected in the presence of progressively increasing levels of jamming power. GPS, Galileo, and Beidou signals were processed with the different approaches that collectively highlighted the benefits of combining interference mitigation and FDE. The combined use of pre-correlation mitigation techniques together with FDE allowed the receiver to provide a reliable navigation solution even in the presence of strong interference. In particular, for the multi-constellation case using GPS and Galileo in which time domain mitigation techniques were applied, a reliable availability of about 94% was achieved. This is because of the time domain techniques adopted and their ability to mitigate the effects of the specific type of jammer used in these tests. On the other hand, the use of a mitigation technique which is not effective at removing interference may lead to a reduction of the number of reliable solutions. The use of multi-layer defense improves the performance of the GNSS receiver, particularly its horizontal position accuracy. Standard deviation values between 1.5 and 3.3 meters were been observed for the multi-constellation solutions with the time domain techniques used in Test 1. By contrast, no significant improvements were observed when using a frequency domain technique. Interference mitigation allows the receiver to track more signals despite high levels of jamming power. This condition guarantees a higher redundancy of GNSS measurements that can be effectively exploited by FDE. Multi-constellation solutions will yield additional improvements in measurement redundancy and will increase the reliability and availability of the final navigational solutions.

AUTHOR CONTRIBUTIONS

Dr. Gioia contributed to the theoretical developments and to the analysis of the reliability scheme. Dr. Borio contributed to the theoretical developments and to the analysis of robust interference mitigation strategies. Both authors drafted and reviewed the manuscript.

CONFLICT OF INTEREST

The authors declare no potential conflict of interests.

REFERENCES

- Angus, J. E. (2006). RAIM with multiple faults. *NAVIGATION*, 53(4), 249–257. <https://doi.org/10.1002/j.2161-4296.2006.tb00387.x>
- Betz, J.W. (2001). Effect of partial-band interference on receiver estimation of C/N0: Theory. *Proc. of the National Technical Meeting of the Institute of Navigation (NTM 2008)*, San Diego, CA. 817–828. <https://www.ion.org/publications/abstract.cfm?articleID=195>
- Betz, J. W., & Kolodziejksi, K. R. (2009). Generalized theory of code tracking with an early-late discriminator part i: Lower bound and coherent processing. *IEEE Transactions on Aerospace and Electronic Systems*, 45(4), 1538–1556. <https://doi.org/10.1109/TAES.2009.5310316>
- Borio, D., & Gioia, C. (2021). GNSS interference mitigation: A measurement and position domain assessment. *NAVIGATION*, 68(1), 93–114. <https://doi.org/10.1002/navi.391>
- Borio, D., Lo Presti, L., & Mulassano, P. (2006). Spectral separation coefficients for digital GNSS receivers. *Proc. of the 14th European Signal Processing Conference (EUSIPCO 2006)*, Florence, Italy. 1–5. <https://www.eurasip.org/Proceedings/Eusipco/Eusipco2006/papers/1568982013.pdf>

- Brown, A. K. (1987). Receiver autonomous integrity monitoring using a 24-satellite GPS constellation. *Proc. of the 1st Technical Meeting of the Satellite Division of the Institute of Navigation (ION GPS 1987)*, Colorado Springs, CO. 256–262. <https://www.ion.org/publications/abstract.cfm?articleID=11922>
- Dovis, F. (Ed.). (2015). *GNSS interference threats and countermeasures*. Artech House.
- Gioia, C. (2014). *GNSS navigation in difficult environments: Hybridization and reliability* [PhD Thesis, University Parthenope of Naples], Naples, Italy. Retrieved from https://pang.uniparthenope.it/sites/default/files/PhD_thesis_CG.pdf
- Gioia, C., & Borio, D. (2016). A statistical characterization of the galileo-to-GPS inter-system bias. *Journal of Geodesy*, 90, 1279–1291. <https://doi.org/10.1007/s00190-016-0925-6>
- Hewitson, S., & Wang, J. (2006). GNSS receiver autonomous integrity monitoring (RAIM) performance analysis. *GPS Solutions*, 10, 155–170. <https://doi.org/10.1007/s10291-005-0016-2>
- Kaplan, E. D., & Hegarty, C. (Eds.). (2005). *Understanding GPS: Principles and applications* (Second Edition ed.). Artech House.
- Klobuchar, J. A. (1987). Ionospheric time-delay algorithm for single-frequency GPS users. *IEEE Transactions on Aerospace and Electronic Systems*, AES-23(3), 325–331. <https://doi.org/10.1109/TAES.1987.310829>
- Kuusniemi, H. (2005). *User-level reliability and quality monitoring in satellite-based personal navigation* [Unpublished doctoral dissertation]. Tampere University of Technology, Finland. Publication 544. https://www.researchgate.net/publication/242381097_User-Level_Reliability_and_Quality_Monitoring_in_Satellite-Based_Personal_Navigation
- Kuusniemi, H., Wieser, A., Lachapelle, G., & Takala, J. (2007). User-level reliability monitoring in urban personal satellite-navigation. *IEEE Transactions on Aerospace and Electronic Systems*, 43(4), 1305–1318. <https://doi.org/10.1109/TAES.2007.4441741>
- Pärlin, K., & Riihonen, T. (2020). Analog mitigation of frequency-modulated interference for improved GNSS reception. *Proc. of the International Conference on Localization and GNSS (ICL-GNSS 2020)* (p. 1–6). <https://doi.org/10.1109/ICL-GNSS49876.2020.9115518>
- Petovello, M. (2003). *Real-time integration of a tactical-grade IMU and GPS for high-accuracy positioning and navigation*. [Unpublished doctoral dissertation]. University of Calgary, Department of Geomatics Engineering. UCGE Report No. 20173. <https://prism.ucalgary.ca/handle/1880/42707>
- Raimondi, M., Macabiau, C., & Julien, O. (2008). Frequency domain adaptive filtering against pulsed interference: Performance analysis over Europe. *Proc. of the National Technical Meeting of the Institute of Navigation (NTM 2008)*, San Diego, CA. 164–176 <https://www.ion.org/publications/abstract.cfm?articleID=7674>
- RTCA Special Committee 159. (2001). *DO-229C - Minimum operational performance standards for global positioning system/wide area augmentation system airborne equipment* (Tech. Rep. No. DO-229D). RTCA.
- Van Dierendonck, A. (1996). Ch. 5, GPS receivers. In B. W. Parkinson & J. J. Spilker Jr. (Eds.), *Global positioning system theory and applications* (Vol. 1, p. 329–407). American Institute of Aeronautics & Astronautics. <https://doi.org/10.2514/5.9781600866388.0329.0407>
- Walter, T., & Enge, P. (1995). Weighted RAIM for precision approach. *Proc. of the 8th International Technical Meeting of the Satellite Division of the Institute of Navigation (ION GPS 1995)*, Palm Springs, CA. 1995–2004. <https://www.ion.org/publications/abstract.cfm?articleID=2524>
- Zhang, X., Xu, M., & Zhang, Z. (2020). Robust GNSS estimation using factor graphs, modified gaussian mixture model and a transformed domain method. *Proc. of the International Technical Meeting of the Institute of Navigation (ITM 2020)*, San Diego, CA. 745–749. <https://doi.org/10.33012/2020.17175>

How to cite this article: Gioia, C., & Borio, D. (2023). Multi-layered multi-constellation global navigation satellite system interference mitigation. *NAVIGATION*, 70(4). <https://doi.org/10.33012/navi.596>